Analytica Chimica Acta 1142 (2021) 99–107

Contents lists available at ScienceDirect

Analytica Chimica Acta

journal homepage: www.elsevier.com/locate/aca

Electro-enhanced solid-phase microextraction with covalent organic framework modified stainless steel fiber for efficient adsorption of bisphenol A

Yue-Hong Pang *, Yu-Ying Huang , Xiao-Fang Shen , Yi-Ying Wang

State Key Laboratory of Food Science and Technology, School of Food Science and Technology, Jiangnan University, Wuxi, 214122, China

HIGHLIGHTS

- Covalent organic framework DQTP was grown *in situ* on stainless steel wire via Schiff base reaction.
- Extraction efficiency of SPME was enhanced by the external electrical field with shorter extraction time.
- The developed EE-SPME coupled with GC-FID method was applied to determine bisphenol A in extracts of food packagings.

GRAPHICAL ABSTRACT

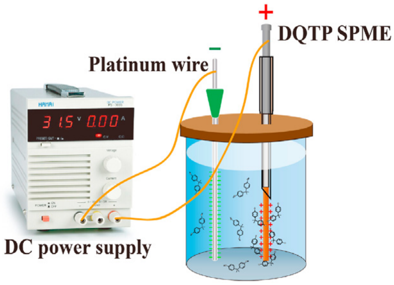

ARTICLE INFO

Article history:
Received 10 July 2020
Received in revised form
24 October 2020
Accepted 31 October 2020
Available online 5 November 2020

Keywords:
Covalent organic framework
Electro-enhanced
Solid-phase microextraction
Bisphenol A

ABSTRACT

In this work, electro-enhanced solid-phase microextraction (EE-SPME) and covalent organic framework (COF) were adopted to improve the extraction efficiency. A conductive COF synthesized of 2,6-diaminoanthraquinone (DQ) and 1,3,5-triformylphloroglucinol (TP) was *in situ* bonded to the stainless steel wire via facile solution-phase approach and used as the EE-SPME fiber coating to preconcentrate a typical endocrine disruptor bisphenol A (BPA). Compared with conventional SPME, the DQTP bonded fiber coupled with EE-SPME device exhibited higher extraction efficiency and achieved extraction equilibrium within 10 min. The proposed approach based on EE-SPME and gas chromatography coupled with flame ionization detector gave a linear range of 0.05–10 $\mu g\ mL^{-1}$ and detection limit of 3 $\mu g\ L^{-1}$ (S/N = 3) with good precision (<6.7%) and reproducibility (<7.1%) spiked with 0.1, 0.5, 1.0 $\mu g\ mL^{-1}$ BPA. Quantitative determination of BPA in extracts of food packagings (mineral water bottles, milk boxes and milk tea cups) was achieved with recoveries from 88.6 to 118.0%.

1. Introduction

Solid-phase microextraction (SPME) is a distinguished environmentally friendly sampling technology introduced in the 1990s by Prof. Pawliszyn, enabling sampling, separation, pretreatment and enrichment in a solvent-free and simple operation [1–3]. Owing to its convenience and simplicity, SPME has been employed in environmental [4–6], food [7–9], and biological [10–13] analyses. The SPME procedure involves the sorption of the target analytes onto the surface of a miniaturized device coated with a dimensionally small extraction phase [14]. The general extraction principle depends on the partitioning equilibrium of the analytes between the sample matrix and the extraction phase via passive

---

* Corresponding author.
E-mail address: yhpang@jiangnan.edu.cn (Y.-H. Pang).

https://doi.org/10.1016/j.aca.2020.10.061

diffusion, which requires time-consuming process that undoubtedly undermines the simplicity and rapidity of SPME [2]. Especially for analytes with high affinity for water, conventional SPME technique has the disadvantage of low extraction efficiency of polar or ionic compounds.

To overcome this limitation, various auxiliary technologies have been introduced to improve the extraction efficiency. As early as 1963, the idea of separating analytes using an electric field in combination with a solid acceptor phase was put forward, and then several research groups proposed an electro-enhanced SPME (EE-SPME) approach, in which an electrical potential was applied to the SPME fiber to accelerate transfer of charged analytes from samples to the fiber surface via electrostatic interaction [15]. To date, EE-SPME method has been found to be suitable for the enhanced extraction of protonated or deprotonated analytes. Mousa et al. [16] and Xu et al. [17] applied commercial SPME fibers (polydimethylsiloxane (PDMS), polydimethylsiloxane/divinylbenzene (PDMS/DVB), carbowax/polydimethylsiloxane and divinylbenzene/carbowax/polydimethylsiloxane) as working electrodes for the extraction of phthalate esters, bisphenol A and amphetamines. These types of coating materials suffer from poor conductivity and low extraction efficiency to strong polar and ionic compounds. However, there are a few different attempts on the development of EE-SPME fiber coating such as molecularly imprinted polypyrrole/multi-walled carbon nanotubes [18], ordered mesoporous carbon [19] and three-dimensional graphene [20]. In order to maximize the EE-SPME efficiency, it is still a challenge to find suitable fiber coating materials with excellent conductivity, superior adsorption capacity and high affinity towards target analytes for the EE-SPME application.

The development of covalent organic frameworks (COFs) based SPME fiber materials with superior characteristics has been of extensive interest. COFs are a new class of two-dimensional porous crystalline materials in which organic building blocks are linked into framework structures with periodic skeletons and ordered pores via strong covalent bonds [21–23]. The unique structure of COFs gives them a variety of properties such as tunable porous structure, large surface areas, low density, good chemical and thermal stability [24], which render them an alternative as coating for SPME to extract efficiently some contaminants [25–27]. Our group previously developed COFs bonded wires as SPME fibers to extract 16 polycyclic aromatic hydrocarbons and 11 phthalate esters with high extraction efficiency [28,29]. DQTP, a β-ketoenamine-linked COF that was synthesized by 2,6-diaminoanthraquinone (DQ) and 1,3,5-triformylphloroglucinol (TP), has great potential for the extraction of some aromatic compounds via π-π stacking interaction and tunable size matching [30]. Its two-dimensional layered architecture and β-ketoenamine linking relative to an electroactive monomer DQ make it has shown promising proton conductivity [31–33], we have reason to speculate that DQTP is potentially useful for the EE-SPME coating.

Bisphenol A (BPA) is a primary additive in polycarbonates and epoxy resins which are widely used in the manufacture of plastic food containers, and an endocrine disrupting compound that arouses abnormal activity and engenders irreversible damage to living organisms. Herein, we reported *in situ* growth of DQTP on stainless steel wire (SSW) as SPME fiber via facile solution-phase approach based on Schiff base reaction and investigated its performance for the EE-SPME. Considering that BPA with two phenolic hydroxyl groups tends to deprotonate under certain pH and potential, we used it as an example for similar polar or ionic analytes. The EE-SPME technology combined with gas chromatography coupled with flame ionization detector (GC-FID) has been developed and successfully applied for the extraction and determination of BPA in extracts of food packagings (mineral water bottles, milk boxes and milk tea cups).

2. Experimental

2.1. Chemicals and materials

All chemicals used were at least of analytical grade. BPA standard (purity 99.0%) was obtained from J&K Chemical (Beijing, China). TP, DQ and chromatographic grade methanol were purchased from Macklin Biochemical (Shanghai, China). N,N-dimethylformamide (DMF), nitric acid, hydrochloric acid, acetone, and acetic acid were purchased from Sinopharm (Shanghai, China). The 5 μL gas chromatograph microsyringes and SSW (23 cm × 0.35 mm) were purchased from High Pigeon (Shanghai, China). The stock solution of BPA at 1000 μg mL^{-1} was prepared in methanol and stored at −20 °C. 10 μg mL^{-1} of standard solution of BPA was obtained by step-by-step dilution of the stock solution with methanol. Working standard solution of BPA was prepared by diluting 10 μg mL^{-1} of BPA standard solution with deionized water.

2.2. Instrumentation

All experiments were carried out at room temperature. The electrochemical behavior of BPA and electrochemical characteristics of DQTP were carried out on CHI660C electrochemical workstation (CH Instruments, Shanghai, China). The morphology of the fiber coating was obtained on a SU8100 scanning electron microscope (SEM) (Hitachi, Tokyo, Japan). Fourier transform-infrared (FT-IR) spectroscopy was recorded on an IS10 FT-IR spectrophotometer (Nicolet, Madison, Wisconsin, USA) and thermogravimetric analysis (TGA) was conducted on TGA2 instrument (Mettler Toledo, Zurich, Switzerland). The X-ray photoelectron spectroscopy (XPS) measurements were performed on Thermo K-Alpha (Thermo Scientific, Waltham, Massachusetts, USA). N_2 adsorption experiments were performed on an Autosorb-iQ analyzer (Quantachrome, Boynton Beach, Florida, USA). EE-SPME experiments were performed in a variable voltage DC power supply purchased from HYELEC (Hangzhou, China). Deionized water (18.2 MΩ·cm, 25 °C) was obtained from a Milli-Q Integral Cabinet 3 system (Millipore, Bedford, Massachusetts, USA). The analysis of BPA was conducted on a GC-2030 system (Shimadzu, Kyoto, Japan) coupled with FID. The capillary column used for separation was HP-5 (30 m × 0.25 mm × 0.25 μm) (Agilent, Palo Alto, California, USA). The injector was operated in the pulsed splitless mode with injector temperature 280 °C. The column temperature program used for the separation was as follows: initial column temperature maintained at 150 °C (held for 2 min), 15 °C min^{-1} to 260 °C (held for 2 min). The detector temperature was set at 300 °C.

2.3. Fabrication of the DQTP bonded SPME fiber

The procedure of DQTP bonding SSW as SPME fiber is according to DeBlase et al. [31] with minor modification. Prior to the fabrication of the DQTP bonded SPME fiber, one end of a SSW was etched by aqua regia for 10 min to obtain a rough surface as a substrate for the preparation of a SPME fiber. Then the etched part was rinsed thoroughly with deionized water and dried in air. The dried etched end was immersed into a solution containing DMF (3.2 mL) and DQ (17.0 mg, 0.071 mmol) in a glass tube at 90 °C. Subsequently, 1 mL of DMF solution containing TP (10.0 mg, 0.048 mmol) and acetic acid (50 μL, 6 M) was added slowly over the course of 1 h via syringe. After the addition, the reaction was allowed to water bath at 90 °C for an additional 3 h. The obtained

DQTP bonded fiber was washed with deionized water and acetone to remove the residual ligands and dried in a vacuum oven at 85 °C for 4 h. Finally, the DQTP bonded fiber was assembled into the microsyringe and aged for 30 min in the GC injector at 300 °C before each extraction.

2.4. Pretreatment of samples

Food packagings (mineral water bottles, milk boxes and milk tea cups) were collected from the local supermarket (Wuxi, China). All samples were cut into small pieces and washed three times with deionized water. Then, 1.0 g of each sample and 10 mL of methanol were placed in a brown glass vial, ultrasonicated for 10 min and stirred at 50 °C for 6 h. After cooling at room temperature, each mixture was filtered with filter membrane and the extract was kept at 4 °C. The 0.1 mL of extract was transferred into a sample vial and diluted with 0.01 mol/L phosphate buffer solution (PBS, pH 4) to obtain 10 mL sample solution. Subsequently, EE-SPME procedure was applied to extract BPA from extracts of pretreated food packagings.

3. Results and discussions

3.1. The design of DQTP bonded fiber for EE-SPME of BPA

The β-ketoenamine-linked COF DQTP was *in situ* synthesized on SSW via facile solution-phase approach based on Schiff base reaction for EE-SPME. The detailed synthesis process for DQTP bonded SPME fiber is illustrated in Scheme 1A. Monomer DQ was grafted on the SSW via the chelate reaction with the metal ions on the rough surface of etched SSW. Another monomer TP was introduced to condensate with DQ via Schiff base reaction to form DQTP on the SSW. After aged at GC injector, we applied the DQTP bonded fiber as a promising candidate for EE-SPME of typical endocrine disrupting compound BPA from extracts of food packagings (Scheme 1B). The successfully fabricated DQTP bonded fiber and a platinum wire were inserted in the sample solution to establish a complete electrical circuit system. Application of potential made the SPME fiber positively charged so that improving the extraction of negatively charged BPA formed by deprotonation in the electric field. Owing to the synergistic effect of π-π conjugate aggregation, hydrogen bonding effect and complementary charge interaction, BPA was extracted onto the fiber from the liquid phase. After the extraction, the fiber was removed from the vial and thermally desorbed in the GC injector for GC analysis, where the peak obtained is employed as the analytical signal for BPA.

3.2. Characterization of the DQTP bonded SPME fiber

The SSW was corroded before bonding coating material DQTP. The smooth bare SSW exhibited rough and metallic surface after aqua regia etching (Fig. 1A and C). Then DQTP was introduced to bond on the etched SSW via *in situ* facile solution-phase approach. Enlargement photograph shows the surface of SSW turns orange-red which is consistent with the color of DQTP (Fig. 1B). SEM image further shows the presence of coral-like nanorodes COF coating on the surface of SSW, which leads to the specific surface area being increased substantially (Fig. 1D and E). And the thickness of the DQTP coating is approximately 6.27 μm based on the cross-section measurement result (Fig. 1F).

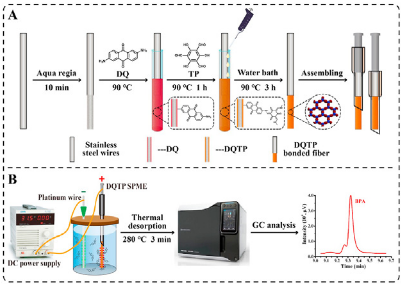

Scheme 1. (A) Illustration of *in situ* fabrication of the DQTP bonded SPME fiber. (B) Schematic of application of EE-SPME-GC for BPA.

The FT-IR spectra of DQTP exhibit the strong characteristic stretching bands at 1567 cm^{-1} (C=C) and 1257 cm^{-1} (C-N), indicating the formation of β-ketoenamine-linked framework structures (Fig. 2A). The C=O stretching peak (1662 cm^{-1}) of TP shifts to 1619 cm^{-1} in the β-ketoenamine, and the N-H stretching peak (3334 cm^{-1}) of DQ weakens. These results indicate the successful condensation of DQ and TP with β-ketoenamine linking. The nitrogen adsorption-desorption isotherm shows that the coating material is microporous structure (Fig. 2B). The total pore volume of the DQTP coating material is 0.3197 cm^3 g^{-1} and a pore diameter is approximately 18 Å, which is close to the simulated DQTP pore size [32]. The DQTP coating is still thermally stable at 350 °C, which is appropriate for application in GC analysis (Fig. S2). The surface chemical composition and bonding environment of DQTP on the SSW were characterized by XPS. The XPS survey spectrum indicates the existence of C, O and N elements (Fig. 2C). Three distinct peaks at 284.79, 286.45 and 288.79 eV are displayed in the C1s high resolution spectra, respectively corresponding to C=C, C-O and C=O (Fig. 2D). The binding energy peaks of O1s high resolution spectra at 531.28 and 532.87 eV are ascribed to the oxygen of −OH and C=O groups (Fig. 2E). And the peak appears at 400.1 eV in the N1s high resolution spectra is assigned to C-N bond (Fig. 2F). The results further prove the synthesis of DQTP on the SSW.

3.3. Optimization of EE-SPME procedure

The DQTP bonded fiber was applied to EE-SPME for quantitative determination of BPA by GC-FID. In EE-SPME procedure, potential parameters such as applied potential, sample pH, extraction time, desorption time and temperature were optimized.

Applied positive potential is an important parameter for EE-SPME for BPA since deprotonated BPA moves towards the positive electrode via electrophoresis and complementary charge interaction. Potentials varying from 0.2 to 0.7 V were investigated. As can be seen from Fig. 3A, the extraction efficiency for BPA increases with the increasing applied potential from 0.2 to 0.5 V. However, we note from the extraction efficiency decreases significantly as the applied potential further increases beyond 0.5 V. This can be attributed to the oxidation reaction of BPA at higher potential (>0.5 V) to form quinones which are insufficient response of GC-FID (Fig. S3). Therefore, applied potential of 0.5 V was selected as the optimum value in subsequent experiments.

Appropriate pH value can accelerate the protonation of BPA, we investigated the pH from 4 to 9. It is observed in Fig. 3B that EE-SPME efficiency gradually decreases with the increase of pH value, which is due to the negative shift of oxidation potential of BPA with the increase of pH value, and BPA is more easily oxidized to quinones in alkaline media [34]. The solubility of weakly acidic BPA will decrease under acidic conditions, thereby increasing the partition coefficient between the fiber coating and the sample solution [35]. Considering that the extraction environment with applied potential is equivalent to the galvanic cell, the corrosion damage of SPME fiber will be caused under a strong acidic condition and the life of fiber will be reduced. Therefore, we chose pH of 4 as the optimum value.

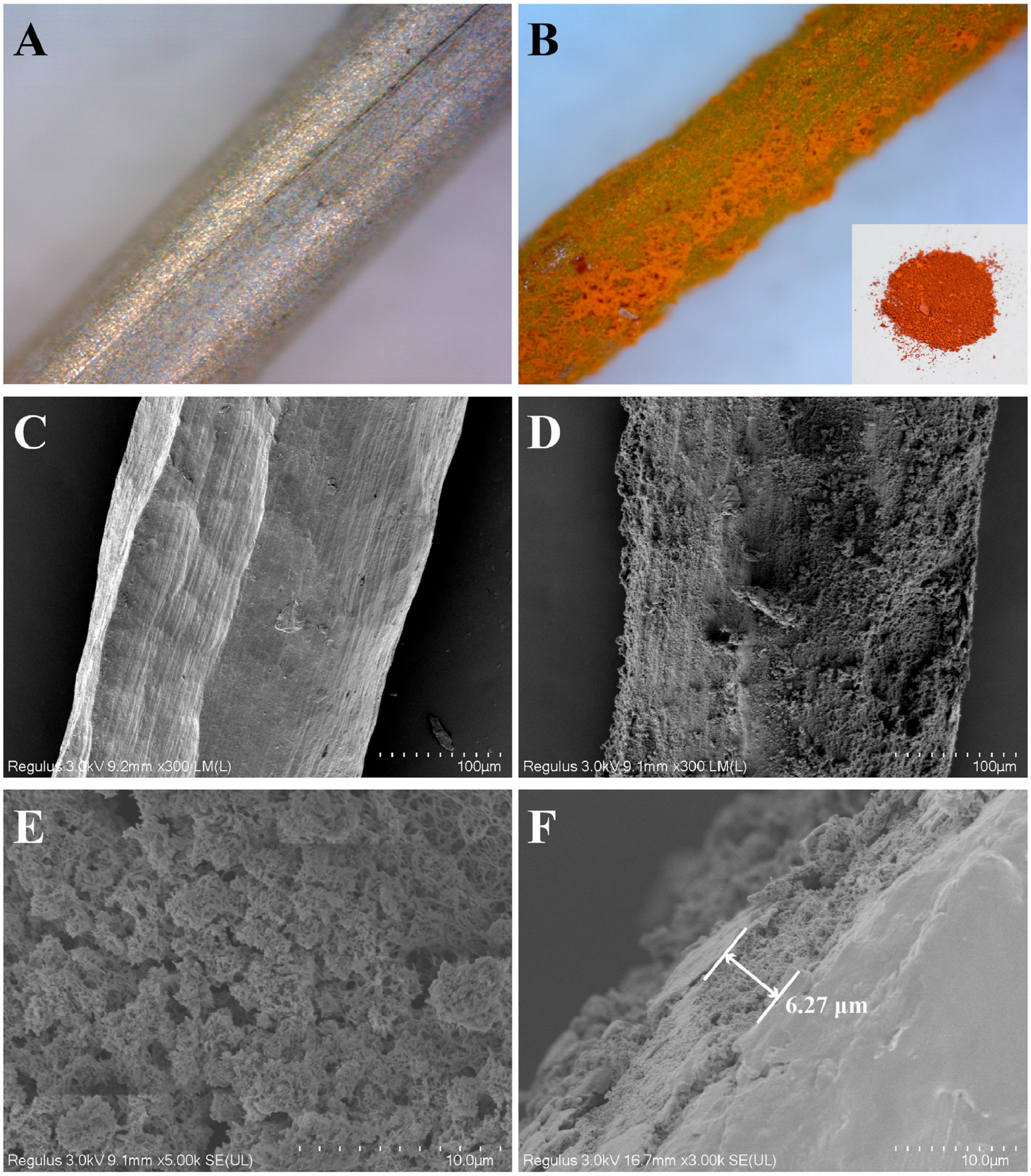

Fig. 1. Magnification of (A) etched SSW fiber and (B) DQTP bonded SPME fiber. (Inset) Photograph of as-synthesized DQTP. SEM images of the (C) etched fiber with magnification at 300 × , the DQTP coated SPME fiber with magnification at (D) 300 × and (E) 5000 × , and (F) cross-section of DQTP bonded SPME fiber.

The effect of extraction time on BPA extraction efficiency was evaluated within 2–20 min (Fig. 3C). The peak area of BPA increases with extraction time up to 10 min and then reaches extraction equilibrium. Hence, 10 min was chosen as the operating extraction time in further experiments. The effects of desorption time and temperature were also studied (Fig. 3D and E). The results show that the desorption time of 3 min with desorption temperature at 280 °C is enough to release the adsorbed BPA from the SPME fiber completely.

3.4. Comparison of different SPME fibers

The researches of extraction efficiency for BPA among the fabricated DQTP bonded fiber (6.27 μm), etched SSW fiber and commercial fibers (30 μm PDMS and 65 μm PDMS/DVB) were conducted under their optimum conditions to evaluate the practical value. As shown in Fig. 4A, the signal of BPA obtained by DQTP coating are higher than those of BPA with etched SSW (24.0-fold), PDMS (9.7-fold) and PDMS/DVB (1.4-fold), respectively. The higher extraction efficiency of as-prepared DQTP bonded fiber for BPA may resulted from the π-π stacking interaction. XPS experiments of DQTP before and after BPA adsorption were investigated to evaluate the bonding environment (Fig. 5A and B). The peak of C=C at 284.77 eV before adsorption shifted to higher binding energy of 284.81 eV after adsorption, indicating that the π-π interaction between DQTP and BPA [36].

Additionally, UV–vis adsorption spectra display a bathochromic shift of the characteristic peak for BPA after adsorption on DQTP, further indicating that the π-π interaction exists during the adsorption of BPA on DQTP (Fig. S4). The suitable pore size of DQTP (18 Å) and hydrogen bonding effect between the hydroxyl group of BPA and the carbonyl groups on the pore walls in DQTP may also play a key role in the extraction process [30,37]. The extraction equilibrium can be achieved in a shorter time after applying the

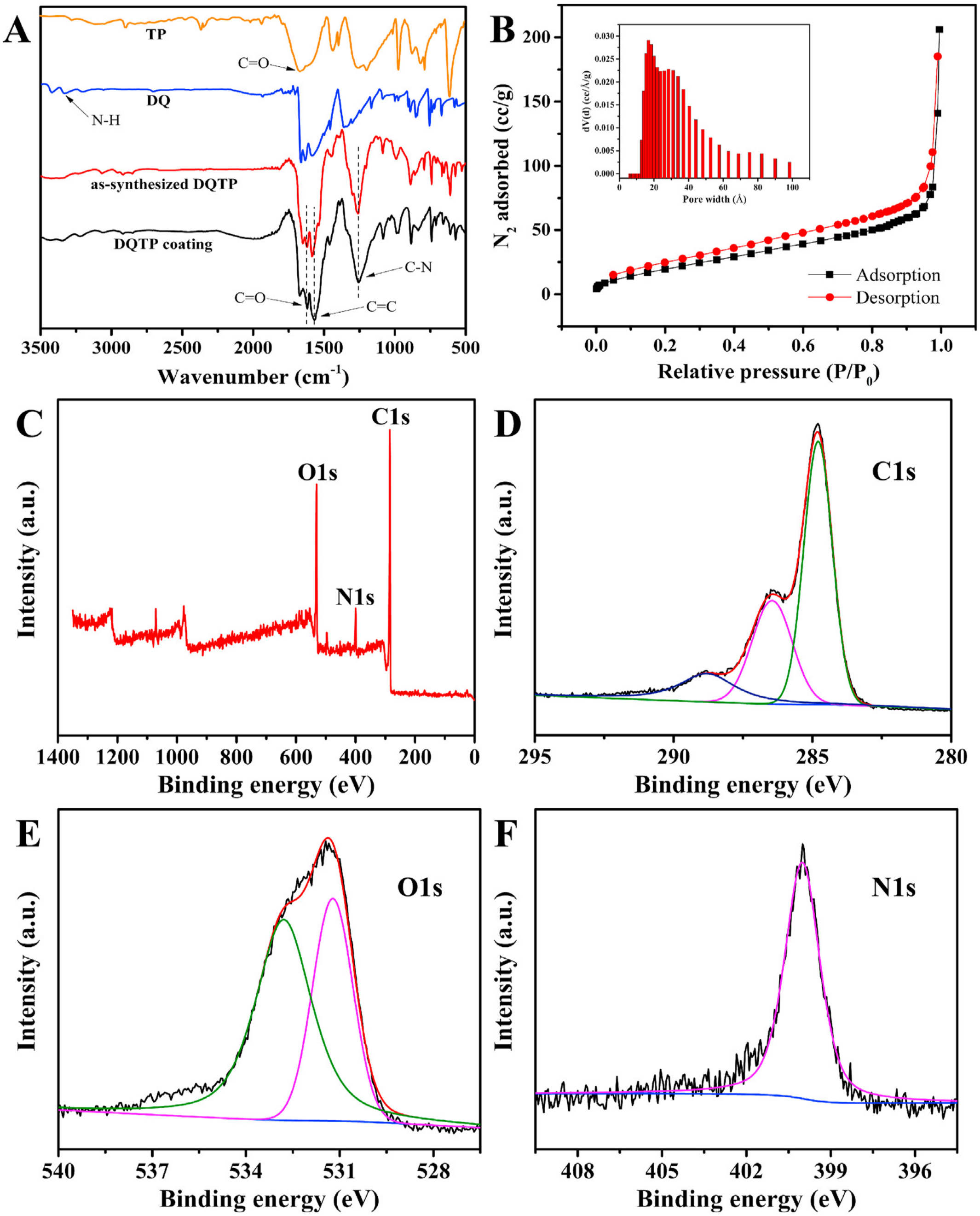

Fig. 2. (A) FT-IR spectra of the TP monomer (orange), DQ monomer (blue), the as-synthesized DQTP (red) and DQTP scraped from the SPME fibers (black). (B) N_2 adsorption-desorption isotherms of DQTP coating at 77 K. (Inset) Pore size distribution of the DQTP coating. XPS survey spectrum (C) and high resolution spectra of C1s (D), O1s (E), N1s (F) of DQTP on the SSW. (For interpretation of the references to color in this figure legend, the reader is referred to the Web version of this article.)

electric field, attributed to the electrostatic interaction occurred between the deprotonated BPA and DQTP (Fig. 4B). Based on the above results, we can assume that the adsorption process between DQTP and analytes is primarily controlled by π-π interaction and hydrogen bonding effect (Fig. 5C), and the supplement of an external electric field on the DQTP fiber can be conducive to enhancing extraction efficiency.

3.5. Method validation

The analytical performance of our prepared DQTP bonded fiber for the EE-SPME of BPA was investigated under the optimized conditions. The developed method exhibited a linear range of 0.05–10 μg mL^{-1} for BPA with R^2 of 0.9962. The detection limit (LOD) (S/N = 3) and the quantification limit (LOQ) (S/N = 10) was calculated to be 3 μg L^{-1} and 11 μg L^{-1}, respectively. The repeatability of the single fiber evaluated by analyzing six replicate extractions of three concentration (0.1, 0.5, 1.0 μg mL^{-1}) of BPA standard solution ranged from 5.2% to 6.7%. Additionally, the reproducibility in relative standard deviation (RSD) was below 7.1% for the three parallel prepared fibers under above three concentration of BPA standard solution. These results endow DQTP bonded fiber EE-SPME with great performance in extraction of bisphenol analogues and potential as a candidate for sample pretreatment. A

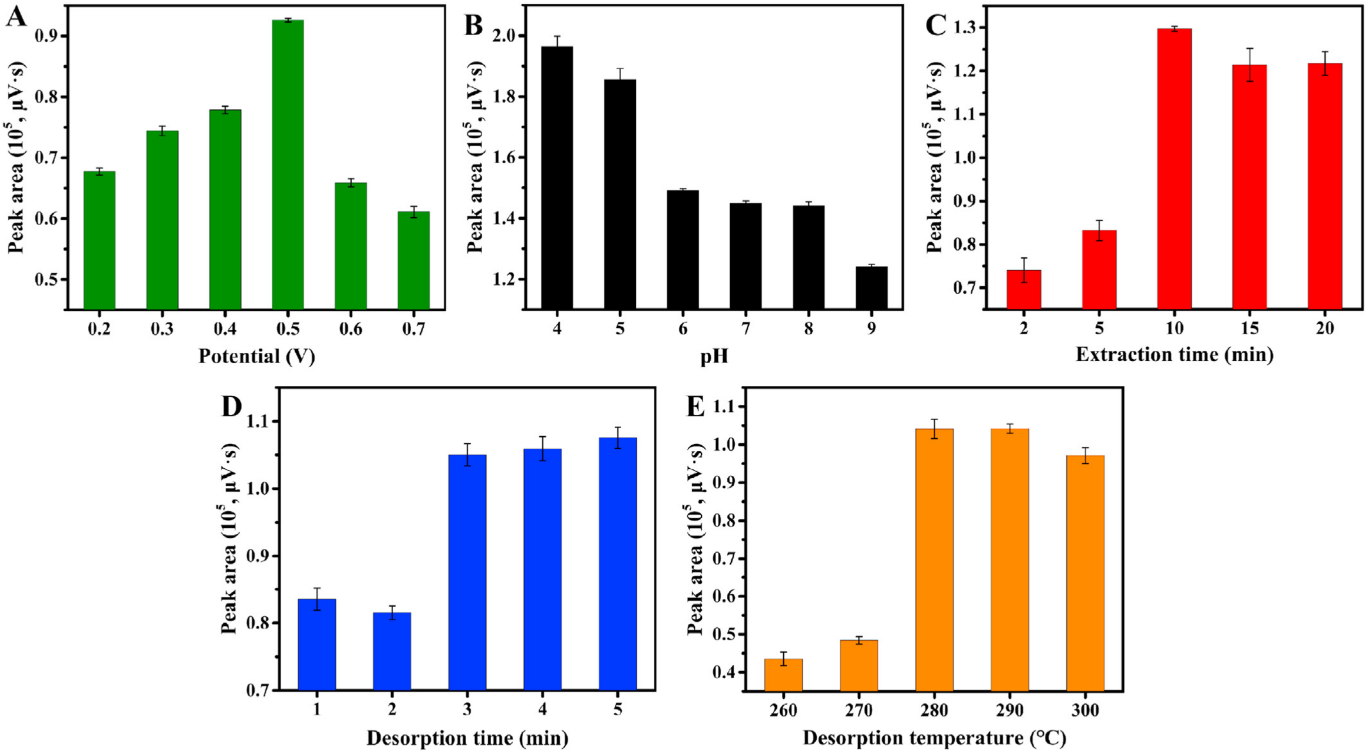

Fig. 3. Effect of experimental conditions on the extraction efficiency of the DQTP bonded fiber for 1 μg mL^{-1} BPA: (A) applied potential (extraction for 10 min in pH 7 PBS solution, desorption at 260 °C for 5 min); (B) pH (applied potential at 0.5 V, extraction for 10 min, desorption at 280 °C for 3 min); (C) extraction time (applied potential at 0.5 V, extraction in pH 4 PBS solution, desorption at 280 °C for 3 min); (D) desorption time (applied potential at 0.5 V, extraction for 10 min in pH 4 PBS solution, desorption at 280 °C); (E) desorption temperature (applied potential at 0.5 V, extraction for 10 min in pH 4 PBS solution, desorption for 3 min).

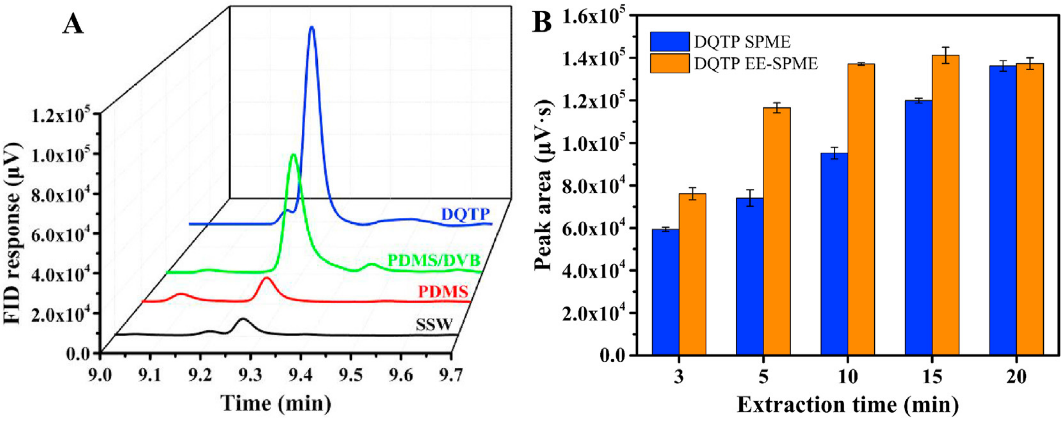

Fig. 4. (A) Chromatograms obtained for the analysis of a 1 μg mL^{-1} BPA standard with different fibers under their optimum conditions: (a) etched SSW fiber (extraction for 10 min in pH 4 PBS solution, desorption at 280 °C for 3 min), (b) commercial PDMS coated fiber (extraction for 40 min in pH 7 PBS solution, desorption at 280 °C for 5 min), (c) commercial PDMS/DVB coated fiber (extraction for 40 min in pH 7 PBS solution, desorption at 270 °C for 5 min) and (d) DQTP bonded SPME fiber (extraction for 20 min in pH 4 PBS solution, desorption at 280 °C for 3 min). (B) Comparison of extraction efficiency of DQTP SPME and DQTP EE-SPME (extraction in pH 4 PBS solution, desorption at 280 °C for 3 min).

comparison of our method with previous SPME methods for the determination of BPA in terms of coating sorbents, amount of material onto the fiber coating, coating preparation time, linear range, LOD, extraction speed and desorption temperature is presented in Table 1. The combination of DQTP bonded fiber with EE-SPME provides a high-efficiency analysis with the extraction in 10 min per sample. Besides, the linear range and LOD of our as-fabricated fiber with less coating materials are comparable with previously reported methods. According to the maximum migration of BPA (0.05 mg kg^{-1}) in food packagings established by European Union [40], the as-proposed method can meet the requirements of BPA detection in real samples.

3.6. *Application to real samples*

After successful validation, the practical applicability of the proposed method for the determination of BPA in extracts of three food packagings (mineral water bottles, milk boxes and milk tea

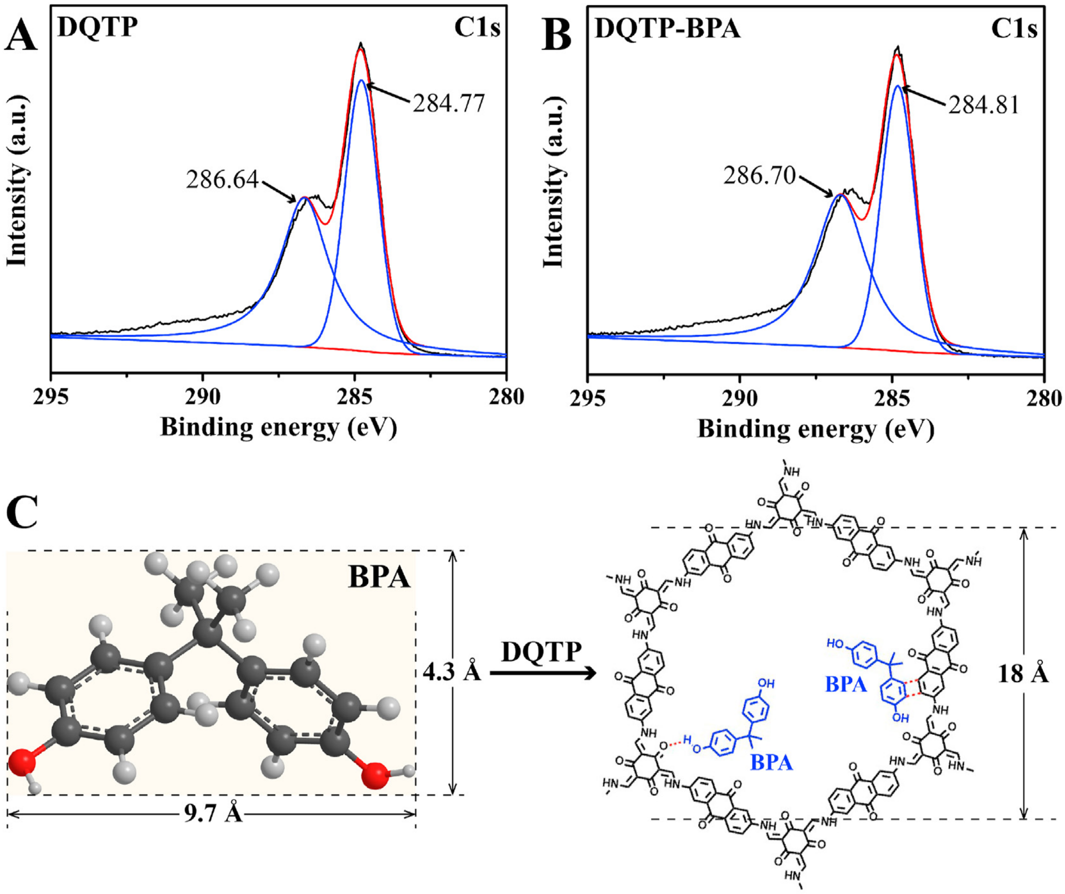

Fig. 5. XPS spectra: C1s of DQTP before (A) and after (B) adsorption of BPA. (C) Illustration of π-π interaction and hydrogen bonding between BPA and DQTP for the adsorption.

Table 1
Comparison with previous reported methods for the determination of BPA.

Method	Coating	Coating preparation time (h)	Linear range (μg L^{-1})	LOD (μg L^{-1})	Extraction time (min)	Desorption temperature (°C)
EE-SPME-GC-FID [20]	Three-dimensional graphene (25 μm)	7.5	100–10000	6	10	280
SPME-GC-MS [38]	Polypyrrole/nanosilica (50 μm)	1.5	0.05–50	0.01	40	280
PT-SPE-GC-MS [39]	Dummy molecularly imprinted polymer (150 mg)	16	50–500	50	–	280
EE-SPME-GC-MS [16]	PDMS (30 μm)	–	2–100	0.096	20	290
EE-SPME-GC-FID (This work)	COF DQTP (6.7 μm)	4	50–10000	3	10	280

Table 2
Recoveries (%), RSD (%, n = 3, in parentheses) and concentrations (mg g^{-1}) of BPA in extracts of different food packagings.

Samples	Concentration	Recovery	
		0.1	1.0
Mineral water bottle 1#	0.02 (2.7)	94.9 (1.5)	117.2 (3.1)
Mineral water bottle 2#	ND[a]	108.3 (7.8)	113.4 (7.2)
Mineral water bottle 3#	ND	88.6 (1.6)	107.0 (6.1)
Milk box 1#	0.03 (2.5)	107.8 (1.8)	89.3 (5.5)
Milk box 2#	0.02 (3.3)	102.7 (1.5)	101.7 (3.6)
Milk tea cup	0.02 (3.3)	90.2 (7.5)	118.0 (1.9)

[a] ND, not detected.

cups) were evaluated (Fig. S5). As shown in Table 2, BPA is actually monitored in mineral water bottles and milk boxes with a maximum concentration of 0.02 mg g^{-1} (RSDs < 2.7) and 0.03 mg g^{-1} (RSDs < 3.3), respectively. And the content of BPA is detected to be 0.02 mg g^{-1} in milk tea cups (RSD = 3.3). The accuracy of the developed method was verified by a recovery study with spiking BPA at two concentration levels (0.1 and 1.0 mg g^{-1}) in extracts of food packagings. The recoveries ranged from 88.6 to 117.2% in mineral water bottles, 89.3–107.8% in milk boxes and 90.2–118.0% in milk tea cups, which indicate that our method is feasible for rapid extraction and accurate determination of BPA in real samples.

4. Conclusions

We reported an *in situ* facile solution-phase approach for the fabrication of DQTP bonded EE-SPME fiber, and its application for the enrichment of BPA in extracts of food packagings. The prepared DQTP bonded fiber coupled with EE-SPME has an acceptable linear range and detection limit with satisfactory reproducibility, precision and recovery. This work provides an efficient preconcentration tool for the enrichment and detection of BPA in real samples, and is expected to extend its application in the extraction of similar polar or ionic analytes.

CRediT authorship contribution statement

Yue-Hong Pang: Conceptualization, Resources, Writing - review & editing, Project administration, Funding acquisition. **Yu-Ying Huang:** Conceptualization, Methodology, Formal analysis, Investigation, Writing - original draft. **Xiao-Fang Shen:** Methodology, Formal analysis, Validation, Investigation. **Yi-Ying Wang:** Validation, Investigation, Data curation.

Declaration of competing interest

The authors declare that they have no known competing financial interests or personal relationships that could have appeared to influence the work reported in this paper.

Acknowledgments

This work was supported by the National Natural Science Foundation of China (21976070) and the Fundamental Research Funds for the Central Universities (JUSRP22003).

Appendix A. Supplementary data

Supplementary data to this article can be found online at https://doi.org/10.1016/j.aca.2020.10.061.

References

[1] M. Llompart, M. Celeiro, C. García-Jares, T. Dagnac, Environmental applications of solid-phase microextraction, Trac. Trends Anal. Chem. 112 (2019) 1–12.
[2] S. Huang, G. Chen, N. Ye, X. Kou, F. Zhu, J. Shen, G. Ouyang, Solid-phase microextraction: an appealing alternative for the determination of endogenous substances–A review, Anal. Chim. Acta 1077 (2019) 67–86.
[3] C.H. Xu, G.S. Chen, Z.H. Xiong, Y.X. Fan, X.C. Wang, Y. Liu, Applications of solid-phase microextraction in food analysis, Trac. Trends Anal. Chem. 80 (2016) 12–29.
[4] L. Liu, W.K. Meng, L. Li, G.J. Xu, X. Wang, L.Z. Chen, M.L. Wang, J.M. Lin, R.S. Zhao, Facile room-temperature synthesis of a spherical mesoporous covalent organic framework for ultrasensitive solid-phase microextraction of phenols prior to gas chromatography-tandem mass spectrometry, Chem. Eng. J. 369 (2019) 920–927.
[5] Y. Jian, J. Deng, H. Zhou, J. Cheng, Fabrication of graphene oxide incorporated polymer monolithic fiber as solid phase microextraction device for determination of organophosphate esters in soil samples, J. Chromatogr. A 1588 (2019) 17–24.
[6] H. Plaisance, P. Mocho, A. Gross, V. Desauziers, Potential of static sampling using solid-phase microextraction for the assessment of formaldehyde sorption on building materials, Atmos. Environ. 218 (2019), 117009.
[7] M. Mei, J. Pang, X. Huang, Q. Luo, Magnetism-reinforced in-tube solid phase microextraction for the online determination of trace heavy metal ions in complex samples, Anal. Chim. Acta 1090 (2019) 82–90.
[8] M. Xu, Z. Jin, Z. Yang, J. Rao, B. Chen, Optimization and validation of in-situ derivatization and headspace solid-phase microextraction for gas chromatography-mass spectrometry analysis of 3-MCPD esters, 2-MCPD esters and glycidyl esters in edible oils via central composite design, Food Chem. 307 (2020) 125542.
[9] T. Sun, M. Wang, D. Wang, Z. Du, Solid-phase microextraction based on nickel-foam@polydopamine followed by ion mobility spectrometry for on-site detection of Sudan dyes in tomato sauce and hot-pot sample, Talanta 207 (2020), 120244.
[10] A. Roszkowska, M. Yu, V. Bessonneau, J. Ings, M. McMaster, R. Smith, L. Bragg, M. Servos, J. Pawliszyn, In vivo solid-phase microextraction sampling combined with metabolomics and toxicological studies for the non-lethal monitoring of the exposome in fish tissue, Environ. Pollut. 249 (2019) 109–115.
[11] B. Hu, B. Zheng, D. Rickert, G.A. Gomez-Rios, B. Bojko, J. Pawliszyn, Z.P. Yao, Direct coupling of solid phase microextraction with electrospray ionization mass spectrometry: a Case study for detection of ketamine in urine, Anal. Chim. Acta 1075 (2019) 112–119.
[12] G. Marrubini, G. Dugheri, G. Cappelli, G. Arcangeli, N. Mucci, P. Appelblad, C. Melzi, A. Speltini, Experimental designs for solid-phase microextraction method development in bioanalysis: a review, Anal. Chim. Acta 1119 (2020) 77–100.
[13] B. Hashemi, P. Zohrabi, M. Shamsipur, Recent developments and applications of different sorbents for SPE and SPME from biological samples, Talanta 187 (2018) 337–347.
[14] K. Murtada, Trends in nanomaterial-based solid-phase microextraction with a focus on environmental applications–A review, Trends Environ. Anal. 25 (2020), e00077.
[15] A. Wuethrich, P.R. Haddad, J.P. Quirino, The electric field–An emerging driver in sample preparation, Trac. Trends Anal. Chem. 80 (2016) 604–611.
[16] A. Mousa, C. Basheer, A.R. Al-Arfaj, Application of electro-enhanced solid-phase microextraction for determination of phthalate esters and bisphenol A in blood and seawater samples, Talanta 115 (2013) 308–313.
[17] R. Xu, H.K. Lee, Application of electro-enhanced solid phase microextraction combined with gas chromatography-mass spectrometry for the determination of tricyclic antidepressants in environmental water samples, J. Chromatogr. A 1350 (2014) 15–22.
[18] X. Liu, X. Wang, F. Tan, H. Zhao, X. Quan, J. Chen, L. Li, An electrochemically enhanced solid-phase microextraction approach based on molecularly imprinted polypyrrole/multi-walled carbon nanotubes composite coating for selective extraction of fluoroquinolones in aqueous samples, Anal. Chim. Acta 727 (2012) 26–33.
[19] J. Zeng, J. Chen, M. Li, F. Subhan, F. Chong, C. Wen, J. Yu, B. Cui, X. Chen, Determination of amphetamines in biological samples using electro enhanced solid-phase microextraction-gas chromatography, J. Chromatogr. B 1000 (2015) 169–175.
[20] J. Zhang, C.Y. Wen, Q. Li, B.E. Meteku, R. Zhao, B. Cui, X. Li, J. Zeng, Electro-enhanced solid-phase microextraction of bisphenol A from thermal papers using a three-dimensional graphene coated fiber, J. Chromatogr. A 1585 (2019) 27–33.
[21] S.Y. Ding, W. Wang, Covalent organic frameworks (COFs): from design to applications, Chem. Soc. Rev. 42 (2013) 548–568.
[22] A.P. Côté, A.I. Benin, N.W. Ockwig, M. O'Keeffe, A.J. Matzger, O.M. Yaghi, Porous, crysstalline, covalent organic frameworks, Science 301 (2005) 1166–1170.
[23] P.J. Waller, F. Gándara, O.M. Yaghi, Chemistry of covalent organic frameworks, Accounts Chem. Res. 48 (2015) 3053–3063.
[24] F. Zhao, H. Liu, S.D.R. Mathe, A. Dong, J. Zhang, Covalent organic frameworks: from materials design to biomedical application, Nanomaterials (Basel) 8 (2017) 15.
[25] J. Pan, S. Jia, G. Li, Y. Hu, Organic building block based microporous network SNW-1 coating fabricated by multilayer interbridging strategy for efficient enrichment of trace volatiles, Anal. Chem. 87 (2015) 3373–3381.
[26] J.X. Guo, H.L. Qian, X. Zhao, C. Yang, X.P. Yan, In situ room-temperature fabrication of a covalent organic framework and its bonded fiber for solid-phase microextraction of polychlorinated biphenyls in aquatic products, J. Mater. Chem. A 7 (2019) 13249–13255.
[27] M. Wu, G. Chen, J. Ma, P. Liu, Q. Jia, Fabrication of cross-linked hydrazone covalent organic frameworks by click chemistry and application to solid phase microextraction, Talanta 161 (2016) 350–358.
[28] T.T. Ma, X.F. Shen, C. Yang, H.L. Qian, Y.H. Pang, X.P. Yan, Covalent immobilization of covalent organic framework on stainless steel wire for solid-phase microextraction GC-MS/MS determination of sixteen polycyclic aromatic hydrocarbons in grilled meat samples, Talanta 201 (2019) 413–418.
[29] Q. Yue, Y.Y. Huang, X.F. Shen, C. Yang, Y.H. Pang, In situ growth of covalent organic framework on titanium fiber for headspace solid-phase microextraction of 11 phthalate esters in vegetables, Food Chem. 318 (2020) 126507.
[30] Y. Song, R. Ma, L. Hao, X. Yang, C. Wang, Q. Wu, Z. Wang, Application of covalent organic framework as the adsorbent for solid-phase extraction of trace levels of pesticide residues prior to high-performance liquid chromatography-ultraviolet detection, J. Chromatogr. A 1572 (2018) 20–26.
[31] C.R. DeBlase, K. Hernández-Burgos, K.E. Silberstein, G.G. Rodríguez-Calero, R.P. Bisbey, H.D. Abruña, W.R. Dichtel, Rapid and efficient redox processes within 2D covalent organic framework thin films, ACS Nano 9 (2015) 3178–3183.
[32] C.R. DeBlase, K.E. Silberstein, T.T. Truong, H.D. Abruna, W.R. Dichtel, β-Ketoenamine-linked covalent organic frameworks capable of pseudocapacitive energy storage, J. Am. Chem. Soc. 135 (2013) 16821–16824.
[33] C. Liang, H. Lin, Q. Wang, E. Shi, S. Zhou, F. Zhang, F. Qu, G. Zhu, A redox-active covalent organic framework for the efficient detection and removal of hydrazine, J. Hazard Mater. 381 (2020), 120983.
[34] P. Butmee, G. Tumcharern, P. Saejueng, D. Stankovic, A. Ortner, J. Jitcharoen, K. Kalcher, A. Samphao, A direct and sensitive electrochemical sensing platform based on ionic liquid functionalized graphene nanoplatelets for the detection of bisphenol A, J. Electroanal. Chem. 833 (2019) 370–379.
[35] L. Qiu, Q. Liu, X. Zeng, Q. Liu, X. Hou, Y. Tian, L. Wu, Sensitive detection of bisphenol A by coupling solid phase microextraction based on monolayer graphene-coated Ag nanoparticles on Si fibers to surface enhanced Raman

spectroscopy, Talanta 187 (2018) 13–18.

[36] Y.Y. Cui, H.B. Ren, C.X. Yang, X.P. Yan, Facile synthesis of hydroxyl enriched microporous organic networks for enhanced adsorption and removal of tetrabromobisphenol A from aqueous solution, Chem. Eng. J. 373 (2019) 606–615.

[37] Y. Li, C.X. Yang, X.P. Yan, Controllable preparation of core-shell magnetic covalent-organic framework nanospheres for efficient adsorption and removal of bisphenols in aqueous solution, Chem. Commun. 53 (2017) 2511–2514.

[38] M.A. Dogaheh, M. Behzadi, Preparation of polypyrrole/nanosilica composite for solid-phase microextraction of bisphenol and phthalates migrated from containers to eye drops and injection solutions, J. Pharm. Anal. 9 (2019) 185–192.

[39] T.A.V. Brigante, L.F.C. Miranda, I.D. de Souza, V.R. Acquaro Junior, M.E.C. Queiroz, Pipette tip dummy molecularly imprinted solid-phase extraction of Bisphenol A from urine samples and analysis by gas chromatography coupled to mass spectrometry, J. Chromatogr. B 1067 (2017) 25–33.

[40] F. Vilarinho, R. Sendón, A. van der Kellen, M.F. Vaz, A.S. Silva, Bisphenol A in food as a result of its migration from food packaging, Trends Food Sci. Technol. 91 (2019) 33–65.